China Ocean Eng., Vol. 28, No. 6, pp. 777 – 790

DOI 10.1007/s13344-014-0060-1, ISSN 0890-5487

Numerical Simulation and Dynamical Analysis for Low Salinity Water Lens in the Expansion Area of the Changjiang Diluted Water*

ZHANG Wen-jing (张文静)[a], ZHU Shou-xian (朱首贤)[b, 1], LI Xun-qiang (李训强)[a], RUAN Kun (阮　鲲)[a], GUAN Wei-bing (管卫兵)[c] and PENG Jian (彭　剑)[a]

[a] *College of Meteorology and Oceanography*, *PLA University of Science and Technology*, *Nanjing 211101*, *China*

[b] *College of Harbor*, *Coastal and Offshore Engineering*, *Hohai University*, *Nanjing 210098*, *China*

[c] *State Key Laboratory of Satellite Ocean Environment Dynamics*, *Second Institute of Oceanography*, *Hangzhou 310012*, *China*

(Received 23 October 2012; received revised form 30 July 2013; accepted 16 December 2013)

ABSTRACT

The low salinity water lenses (LSWLes) in the expansion area of the Changjiang diluted water (CDW) exist in a certain period of time in some years. The impact of realistic river runoff, ocean currents and weather conditions need to be taken into account in the dynamical analysis of LSWL, which is in need of research. In this paper, the POM-*σ*-*z* model is used to set up the numerical model for the expansion of the CDW. Then LSWL in summer 1977 is simulated, and its dynamic mechanism driven by wind, tide, river runoff and the Taiwan Warm Current is also analyzed. The simulated results indicate that the isolated LSWL detaches itself from the CDW near the river mouth, and then moves towards the northeast region outside the Changjiang Estuary. Its maintaining period is from July 26 to August 11. Its formation and development is mainly driven by two factors. One is the strong southeasterly wind lasting for ten days. The other is the vertical tidal mixing during the transition from neap tide to spring tide.

Key words: *Changjiang diluted water*; *low salinity water lens*; *numerical simulation*; *dynamic mechanism*

1. Introduction

The Changjiang River is the largest river in China, and its annual average discharge is about 9322.7×10^8 m^3 (Shen *et al*., 2001). Its huge freshwater spreads to the Changjiang Estuary (CE), the East China Sea (ECS) and the Yellow Sea (YS), and forms a strong plume front. The Changjiang diluted water (CDW) and its plume front make an enormous impact on the current, water mass, sediment movement and environment of the CE, ECS and YS. So they are always the emphases of ocean engineering and physical oceanography research.

Observations also indicate that the CDW is not always continuous, and sometimes there are some isolated low salinity water lenses (LSWLes) , which change the plume front of the CDW. Recently,

* This project was supported by the National Natural Science Foundation of China (Grant Nos. 40906044, 41076048 and 41376012), the Fundamental Research Funds for the Central Universities (Grant No. 2011B05714) and the Doctoral Starting up Foundation of College of Meteorology and Oceanography of the PLA University of Science and Technology, China.

1 Corresponding author. E-mail: zhushouxian@vip.sina.com

some studies on the mechanism of the LSWL have been made. By analysing the observed data in the east of Cheju Island, Lie *et al*. (2003) suggested that CDW patches separated from the shelf shallow area and then were advected offshore toward Cheju Island as a series of LSWLes were affected by south wind in summertime. Under the climatology condition, Chen *et al*. (2008) used the unstructured-grid, Finite-Volume Coastal Ocean Model (FVCOM) to simulate some LSWLes in the sea west of 123° E, and proposed that the detachment of the LSWL is associated with eddies generated by the baroclinic instability across the plume front. Using the Regional Ocean Modeling System (ROMS), Moon *et al*. (2010) simulated the LSWL under the idealized wind, tide and runoff conditions, and suggested that the strengthening of the tidal mixing during spring tide plays an important role in the formation of the LSWL. The analysis of the salinity observation in August of thirteen years (Pu, 2002) showed that LSWLes only existed in seven years. In August of these years, the difference of tides was little, but there was a significant difference among runoff, circumfluence (namely the residual current) and atmospheric conditions. Therefore, it is necessary to make further research of the LSWL under the real runoff, current and atmosphere conditions. In this paper, the real LWSL in summer 1977 is simulated to analyze its characteristics and dynamical mechanism.

2. The Numerical Model for CDW

POM-σ-z mode (Zhang *et al*., 2011) is used in the simulation of the CDW, which is developed from POM (Blumberg and Mellor, 1987). As shown in Fig. 1, σ coordinate is for the current calculation, and the transform is:

$$\sigma_1 = \frac{z-\eta}{H+\eta} = \frac{z-\eta}{D}, \tag{1}$$

where H is the bottom topography, η is the surface elevation, and $D = H + \eta$ is the total water depth. As shown in Fig. 2, σ-z coordinate is for the salinity calculation. The water is divided into two parts in the vertical direction, and $z = -H_0$ is the interface. σ coordinate is used in the water above the interface, and the transform is

$$\begin{cases} \sigma_2 = \dfrac{z-\eta}{H+\eta} & H \le H_0 \\ \sigma_2 = \dfrac{z-\eta}{H_0+\eta} & H > H_0 \end{cases} \tag{2}$$

z coordinate is used in the water below the interface.

The computational domain covers the Bohai Sea, the YS and the ECS. The numerical grids are shown in Fig. 3. The length of the smallest grid near the CE is 1540 m, and that of the largest grid far away from the CE is about 25000 m. In the vertical direction, the current calculation uses 20 σ vertical layers, and the values of σ for these layers are −0.00056, −0.00167, −0.00335, −0.00670, −0.01339, −0.02679, −0.05357, −0.10714, −0.17857, −0.25000, −0.32143, −0.39286, −0.46429, −0.53571, −0.60714, −0.67857, −0.75000, −0.82143, −0.89286, and −0.96429, respectively. The salinity calculation is in σ-z layers, which have eight uniform σ layers in the upper water and 24 z layers in the

lower water, and the interface of these two parts is at the depth of 25 m. The depths of the 24 z layers are 27 m, 30 m, 35 m, 42 m, 50 m, 60 m, 75 m, 100 m, 150 m, 200 m, 300 m, 500 m, 700 m, 1000 m, 1500 m, 2000 m, 2500 m, 3000 m, 3500 m, 4000 m, 4500 m, 5000 m, 5500 m and 6000 m, respectively.

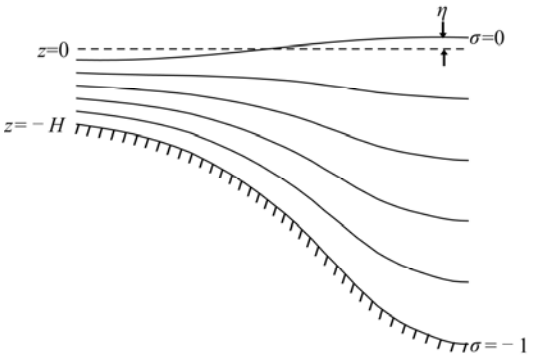

Fig. 1. σ coordinate for the current calculation.

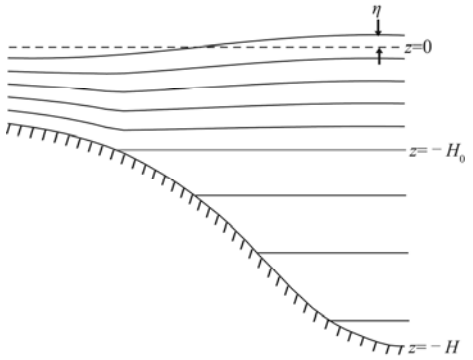

Fig. 2. σ-z coordinate for the salinity calculation.

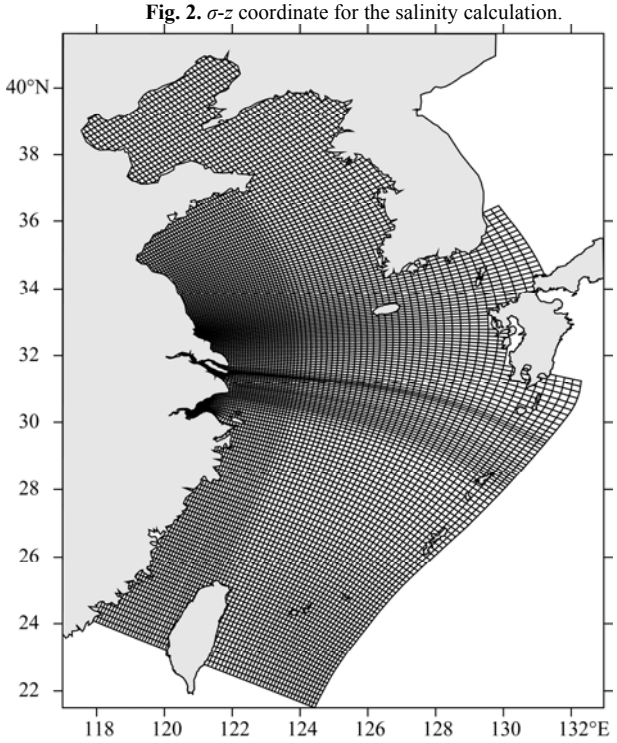

Fig. 3. Calculation area and grid for CDW.

The numerical test of CASE77 is made to simulate the LSWL in summer 1977. CASE77 couples the tidal current and the circumfluence at the open boundary. The tidal current is driven by the harmonic constant of M_2, S_2, K_1, and O_1 tidal constituents. The circumfluence is given in some channels such as influent flux of 2.0 Sv (Sv is $10^6 m^3/s$) in Taiwan Strait, influent flux of 29.9 Sv in Kuroshio Entrance east of Taiwan Island, excurrent flux of 29.4 Sv in Osumi-spit Karma La Strait, and excurrent flux of 2.5 Sv in Tsushima-Korea Strait. The Changjiang River runoff is offered with the

monthly averaged flux in 1977 at Datong Station. The Qiantang River runoff is 2400 m^3/s, which is the climatic average in summer. In order to keep the balance of the total flux, an additional outflow flux is given in Tsushima-Korea Strait, which equals the total runoff of the Changjiang River and the Qiantang River. The wind force is obtained from the NCEP reanalysis of 6-hourly 10-m wind data in 1977. And the climatic average of the salinity and sea temperature in summer is used as the original field data. The coupling calculation of the tidal current and the circumfluence begins on June 10, 1977. Then it runs together with the salinity calculation on June 25, 1977. The sea temperature does not change with time in the calculation. The numerical scheme of CASE77 is similar to that of the previous study (Zhang *et al*., 2011), which introduced more details of the model and its validation.

3. Analysis of the LSWL's Evolution by Numerical Results

Using the same data from the cruise observation in summer 1977, Pu (2002) and Liao *et al*. (2001) both discovered the LSWL. Fig. 4 is the observed surface salinity drawn by Pu (2002), in which there is an isolated LSWL in the northeast outside the CE. The center of the LSWL is at 124° E, 32.9° N, and the value of the center closure isohaline is 24. Fig. 5 is the observed surface salinity drawn by Liao *et al*. (2001), in which there is also an isolated LSWL. But there is another high salinity water lens between the LSWL and the CE. The difference of the two drawings may come from the insufficiency and non- synchronicity of the observation.

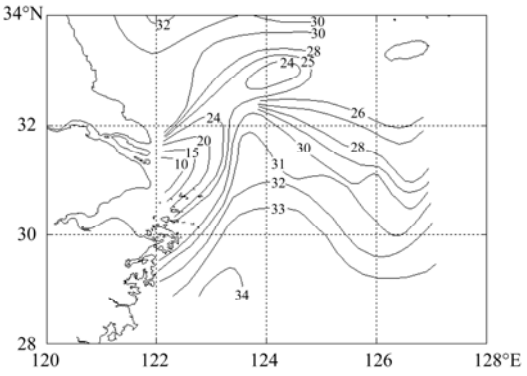

Fig. 4. Distribution of the surface salinity in August 1977 (Pu, 2002).

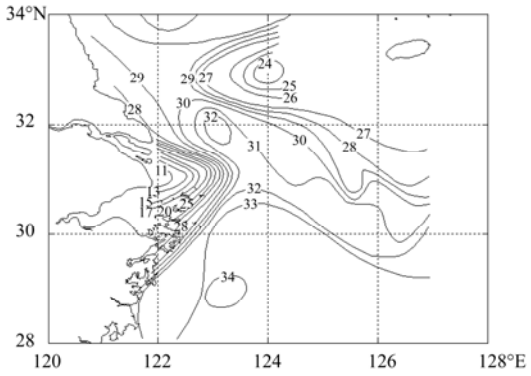

Fig. 5. Distribution of the surface salinity in August 1977 (Liao *et al*., 2001).

The simulation of CASE77 shows that there was an LSWL in the northeast outside the CE from 13:00 July 26 to 11:00 August 11. Fig. 6 gives part of the simulated surface salinity. The CDW spread mainly towards southeast and its northern plume front was located around 32° N on July 22. At 13:00 July 26, the detachment of the LSWL occurred at the interior side of the plume front around 122.2° E, 32° N. The size of the LSWL was 30 km, and its value of the center closure isohaline was 13. From July 26 to August 1, the LSWL moved northeastward quickly with its size gradually enlarging and its value of the central salinity increasing. At 9:00 August 1, the center of the LSWL was located around 123° E, 32.8° N, its size was about 130 km, and its value of central closure isohaline was 24. From

August 1 to 3, the LSWL moved eastward slowly with the size of 100 km, and its central salinity increased gradually. At 20:00 August 3, when its center arrived around 123.3° E, 32.8° N, its size was reduced to 80 km, and the value of the central closure isohaline increased to 26. From 20:00 August 3 to 11:00 August 11, the central position of the LSWL was nearly fixed, and its size gradually decreased to zero as its central salinity increased to 27. After August 11, the surface salinity in the northeast outside the CE had kept a tongue shape until August 25.

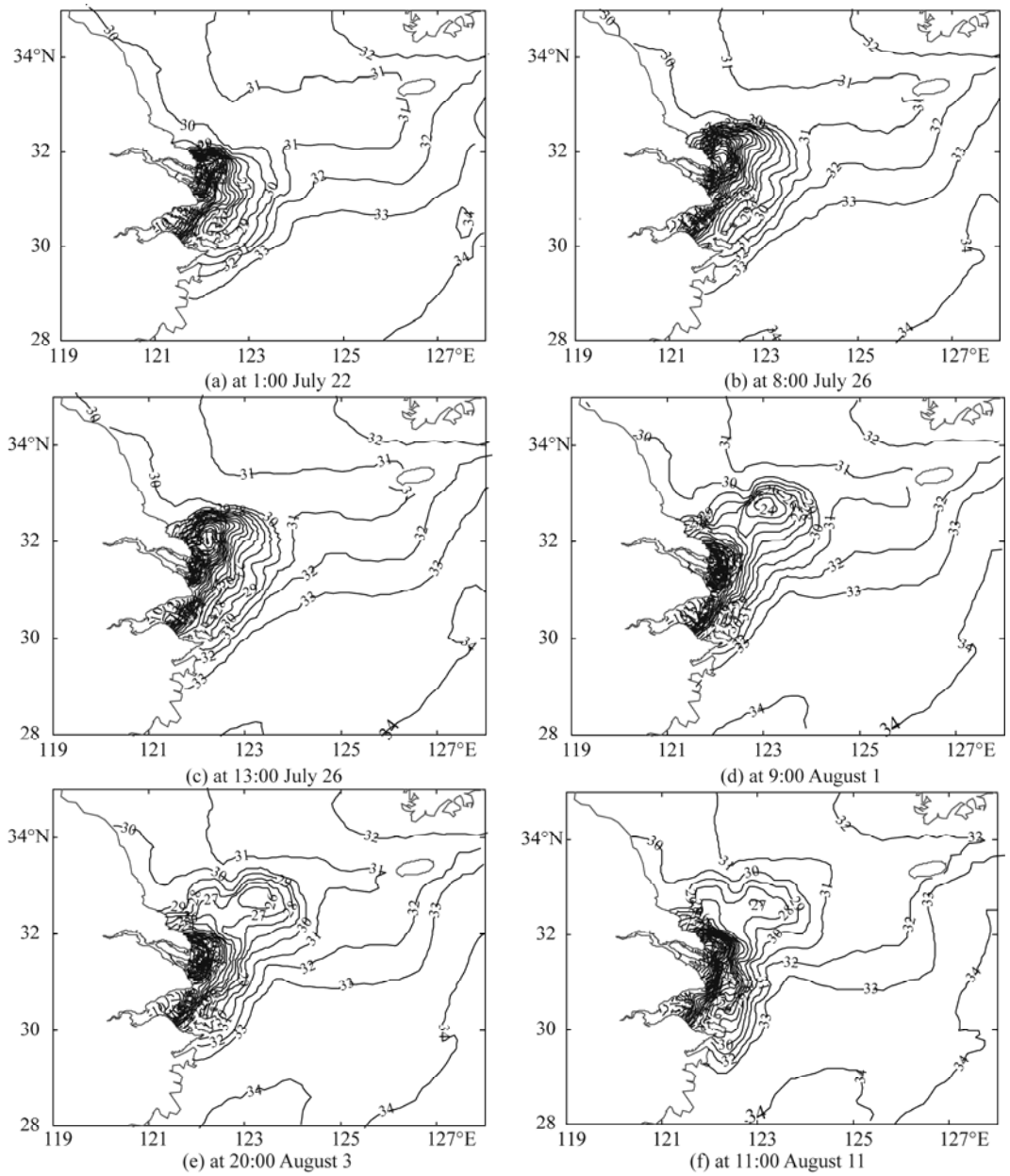

Fig. 6. Simulated surface salinity in CASE77.

4. Analysis of LSWL's Dynamic Mechanism

4.1 Effect of Wind

4.1.1 *Relationships Among the Evolution of Wind, Lagrangian Residual Current and LSWL*

Fig. 7 shows the 5-day averaged wind of NCEP from July 17 to August 15 in 1977. Based on the simulated results of CASE77, Lagrangian residual current (LRC) was calculated. Firstly, LRC of each day was calculated by tracing particles in two M_2 tidal periods. Then, the 5-day averaged LRC was made based on the daily LRC. Fig. 8 shows the 5-day averaged LRC of the sea surface. Although the figurers of wind and LRC from August 16 to 25 were not given, they were also discussed in the following.

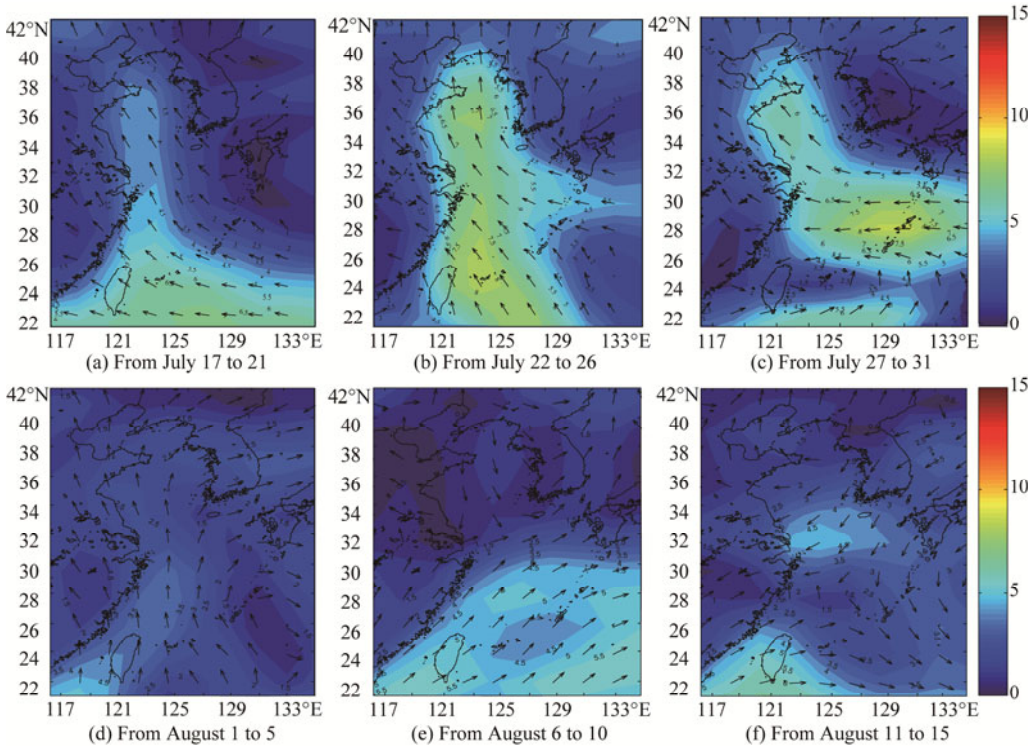

Fig. 7. Variation of the sea surface wind from July 17 to August 15 in 1977 (the vectors represent the wind direction and the color represents the wind speed).

For convenience, we only analyze wind and LRC in the expansion area of the CDW, which is in the range of 121° E−126° E, 30° N−33.5° N. From July 17 to 21, it was controlled by southeastward wind with a mean speed of 4 m/s, and LRC mainly pointed to north or northeast with an average speed of 13 cm/s, while LRC pointed to south or southeast in the range between 122° E and 123° E near the estuary. From July 22 to 31, the wind direction still remained southeastward, but the mean wind speed increased to 6.0−6.5 m/s, and LRC mainly pointed to northeast or north and its mean speed increased to 20 cm/s. From August 1 to 5, it was mainly controlled by southerly wind with a mean speed of 2.5 m/s, but the direction of LRC was not uniform, and it mainly pointed to northeast with a speed of 11 cm/s in the northeast outside the CE. From August 6 to 10, the wind direction was not uniform with a speed of

0.5−4.5 m/s, and the direction of LRC mainly pointed to south with a mean speed of 9 cm/s. From August 11 to 15, it was mainly controlled by the northeasterly wind with a speed of 2.5−4.5 m/s, and the direction of LRC was mainly to south near the estuary and to northwest outside the estuary at an average speed of 11 cm/s. From August 16 to 25, it was still controlled by the northeasterly wind with a speed of 5.0−8.5 m/s, but the direction of LRC was mainly to south near the estuary and to west outside the estuary at an average speed of 20 cm/s.

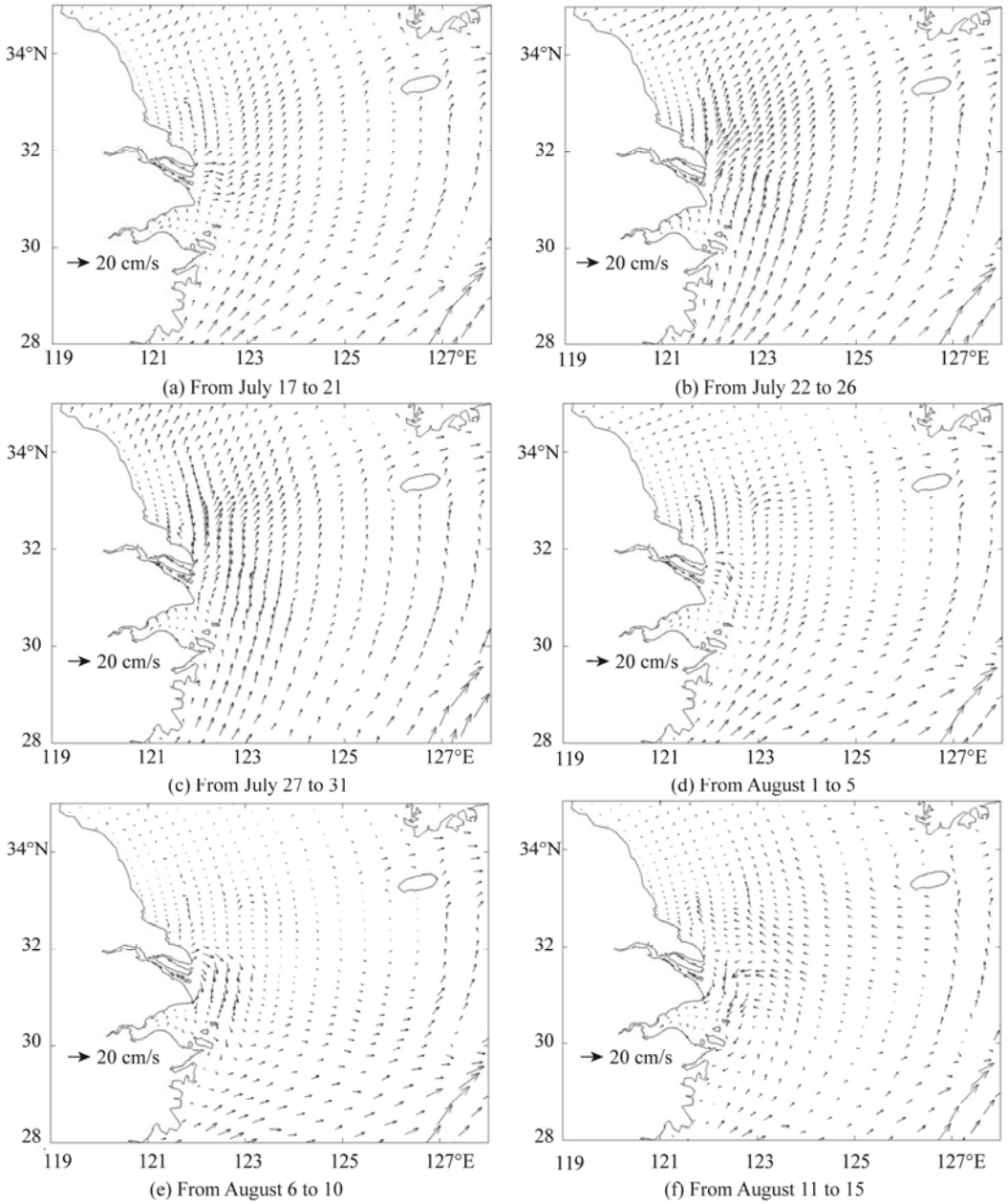

Fig. 8. Distribution of the 5-day mean Lagrangian residual current of the sea surface in CASE77.

There was a close relationship among the evolution of wind, LRC and LSWL. From July 22 to 31, forced by the strong southeasterly wind with a mean speed of 6.0−6.5 m/s, LRC pointed to northeast or north with a high mean speed of 20 cm/s, thus the CDW mainly extended northward. The detachment of the LSWL occurred on July 26, and then the LSWL moved towards northeast with its scale increasing from July 26 to August 1. Fig. 8c shows LRC from July 27 to 31. Its northward speed near 122.5° E was significantly larger than those at its two sides, which can be explained by two mechanisms. Firstly, the wind-induced northerly LRC increased from the deep shelf sea to the shallow estuary. Secondly, the river discharge and density current at sea surface both pointed towards the outside of the river mouth, and then turned to south by the Coriolis force, which was in the opposite direction of the wind-induced Ekman flow. As a result, the northerly LRC in the west of 122.5° E was weak. The nonuniform LRC imposed northward an uneven force on the CDW and cut it off to form the LSWL.

4.1.2 *Numerical Tests by Changing Wind*

Two numerical simulations, namely CASE77a and CASE77b, were conducted to test the effect of the wind on LSWL.

CASE77a used the same model settings like CASE77 except that it got rid of the wind force from July 22. As shown in Fig. 9, the easterly and northeasterly offshore expansion of the CDW in CASE77a was weaker than that in CASE77, and there was not any LSWL.

CASE77b also used the same model settings like CASE77 except that it changed the wind to the climatic mean southerly wind of 4 m/s from July 22. As shown in Fig. 10, the northeasterly offshore expansion of the CDW was also weaker in CASE77b than that in CASE77. There was not any LSWL lasting a long time in the northeast out of the CE. Two small LSWLes happened near the river mouth: the first one was around 122.4° E, 31.8° N with size of 30−35 km from 5:00 July 28 to 7:00 July 30, and the second one was from 4:00 August 12 to 20:00 August 13 with similar characteristics as those of the first one.

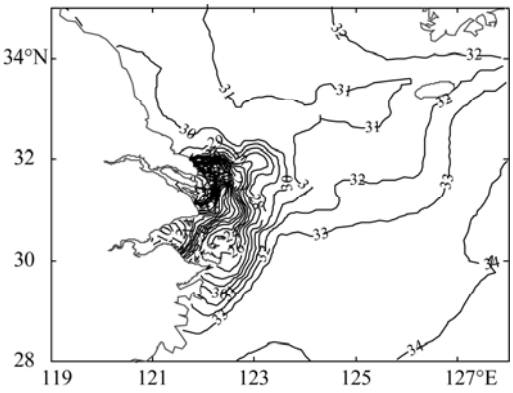

Fig. 9. Simulated surface salinity at 20:00 August 3 in CASE77a.

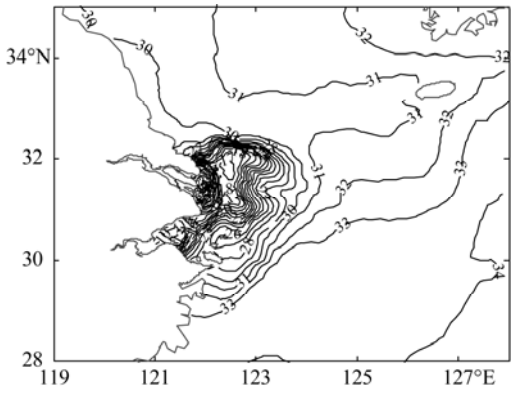

Fig. 10. Simulated surface salinity at 4:00 July 30 in CASE77b.

4.2 Effect of Tide

Three numerical tests, namely CASE77c, CASE77d and CASE77e were conducted to analyze the effect of the tide on the LSWL.

CASE77c used the same model settings like CASE77 except that it switched the tidal force. In CASE77c, from July 22 to July 28, the CDW extended towards north from south. A small LSWL detached at 3:00 July 27 around 122.5° E，32° N with size of 30−40 km, and it had lasted only for 33 hours. From July 28 to August 3, a high salinity tongue was formed around 122.8° E and intruded northward, cutting off the CDW. As shown in Fig. 11, the LSWL was formed at 1:00 August 3 in the northeast out of the CE, and its center was around 123° E, 32.9° N with a size of 70 km. It disappeared at 9:00 August 3, and then regenerated at 5:00 August 4 and lasted until 21:00 August 23. At 23:00 August 6, the third LSWL was detached near the river mouth with size of 70 km. It disappeared at 12:00 August 13, then regenerated at 16:00 August 15 and had lasted until 5:00 August 17.

CASE77d used the same model settings like CASE77 except that in CASE77d only the M_2 tide was considered as the tidal force. In CASE77d, the CDW extended northward from July 22 to July 28, but there was not any LSWL near the river mouth. There were two LSWLes in the northeast out of the CE: one was from 6:00 to 17:00 on August 12 as shown in Fig. 12, and the other was from 21:00 August 17 to 15:00 August 18.

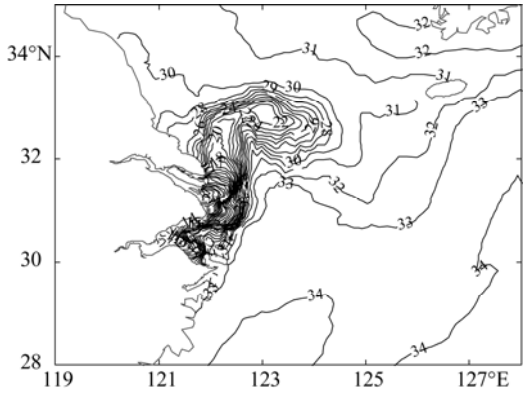

Fig. 11. Simulated surface salinity at 1:00 August 3 in CASE77c.

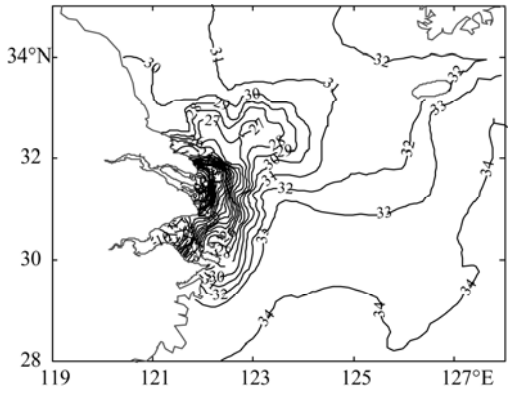

Fig. 12. Simulated surface salinity at 6:00 August 12 in CASE77d.

In the northeast outside the CE, the LSWL had remained until August 23 in CASE77c without any tide force, it had remained less than two days in CASE77d with only M_2 tide force, and it had remained until August 11 in CASE77 with four tides force. It is clear that the tidal force is unfavorable for the maintenance of the LSWL in the northeast outside the CE, which can be explained by the inhibitory action of the tide-induced horizontal mixing. However near the river mouth, the LSWL occurred at 13:00 July 26 in CASE77, and then it developed and moved towards the northeast outside the CE. In CASE77c, a short-lived LSWL appeared near the river mouth from 3:00 July 27 to 12:00 July 28, and there had been not any LSWL in the northeast outside the CE until August 3. In CASE77d, there was not any LSWL near the river mouth. So the combined action of the four tidal constituents was

important to the detachment and development of the LSWL near the river mouth. The tidal table of Lvhuashan Station at 122.617° E, 30.817° N shows that the time from July 26 to August 2 was the transition time from neap tide to spring tide. In CASE77b with the southerly wind of 4 m/s, two LSWLes appeared near the river mouth, one was from July 28 to July 30, and the other was from August 12 to August 13 when the neap tide changed to the spring tide. So it seems that the detachment of the LSWL near the river mouth was related to the salinity variation during the transition of neap tide to spring tide, which was verified by a new experiment of CASE77e.

CASE77e used the same model settings like CASE77 except that it was impacted by southerly wind of 4 m/s and river runoff of 45600 m^3/s which were the typical summertime values. CASE77e eliminated the influence of the variation of wind force and river runoff. In CASE77e, there were two LSWLes near the river mouth: one was from July 28 to 30 as shown in Fig. 13, and the other was from August 12 to 14. A vertical section from 121.97° E, 31.68° N to 123.55° E, 32.64° N was selected to show the salinity variation from neap tide to spring tide, as shown in Fig. 14. There was clear vertical salinity stratification with low-salinity at the surface and with high-salinity at the bottom on July 25 during the neap tide period, and the surface salinity increased from the shallow estuary to the deep shelf sea. As the middle tide arrived, the tide-induced vertical mixing at the shallow water strengthened faster than that at the deep water, so the surface salinity in the shallow water increased faster than that in the deep water on July 28. On July 29, the surface salinity in the shallow water was higher than that in the transition area between the shallow water and the deep water, and thus the LSWL was formed. On the spring tide, the tide-induced vertical mixing kept on strengthening. The salinity in the shallow water was nearly uniform in the vertical direction and the surface salinity in the deep water also increased, thus the surface salinity increased from the shallow water to the deep water again. And the LSWL disappeared on August 1.

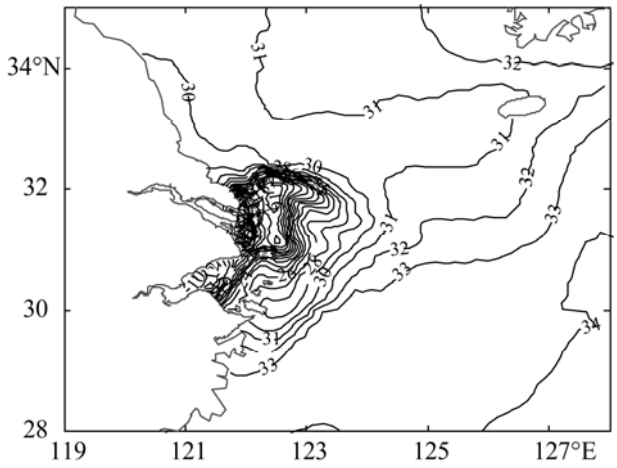

Fig. 13. Simulated surface salinity at 9:00 July 29 in CASE77e.

It is well known that there are fronts of sea temperature in the continental shelf in summer, which are induced by the well-mixed seawater of the shallow nearshore region and the stratified seawater of

the deep offshore region on the impact of tidal vertical mixing (Simpson *et al*., 1974; Huang *et al*., 1996; Lv *et al*., 2007). The mechanism of the LSWL detached by the vertical tidal mixing near the river mouth is similar to that of the tide-induced fronts.

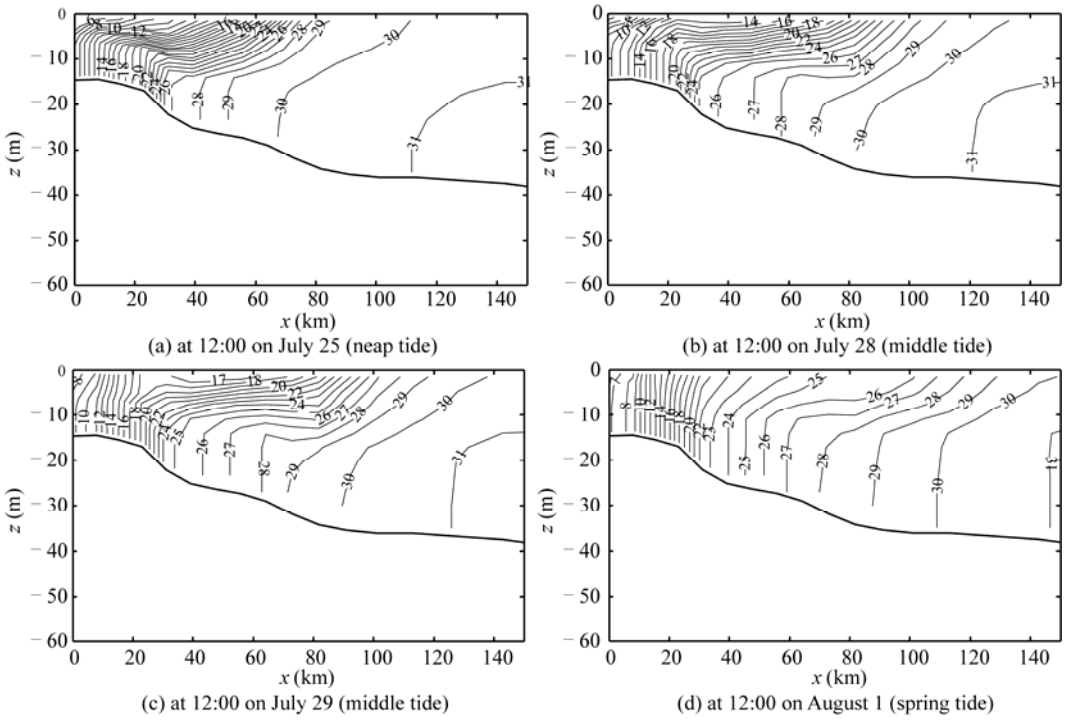

Fig. 14. Simulated vertical distributions of salinity along section in CASE77e.

4.3 Effect of River Runoff

Two numerical tests, namely CASE77f and CASE77g were made to analyze the effect of river runoff on LSWL.

CASE77f used the same model settings like CASE77 except that it doubled the value of Changjiang river runoff. In CASE77f, there was an LSWL forming near the river mouth and moved to the northeast outside the CE from 13:00 July 26 to 20:00 August 12. This LSWL was similar to the one in CASE77 except that its central salinity was 2−6 lower. Fig. 15 gives the characteristics of the LSWL at 20:00 August 3. After August 12, the surface salinity maintained tongue shape in the northeast outside the CE. And two LSWLes appeared in the tongue, one was from 23:00 August 13 to 8:00 August 16, and the other was from 8:00 August 18 to 6:00 August 19.

CASE77g used the same model settings like CASE77 except that it cut the value of Changjiang river runoff in half. In CASE77g, there was an LSWL forming near the river mouth and moved to the northeast outside the CE from 12:00 July 26 to 17:00 August 6. This LSWL was similar to the one in CASE77 except that its central salinity was 2−5 higher and had lasted for 5 days shorter. Fig. 16 gives the characteristics of the LSWL at 20:00 August 3. There was also another LSWL in the northeast outside the CE from 23:00 August 13 to 2:00 August 16.

In the simulations conducted by Zhu and Shen (1997), it was indicated that the variation of river runoff changed only the current speed and the value of salinity outside the CE, rather than the basic characteristics of the current and the expansion of the CDW. In CASE77f and CASE77g, the river runoff did not change the basic characteristics of the CDW or the LSWL, but affected the central salinity and the detachment time of the LSWL.

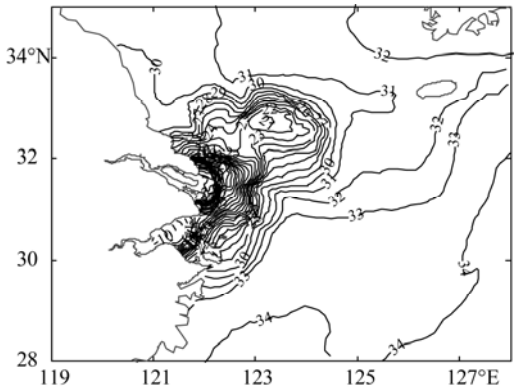

Fig. 15. Simulated surface salinity at 20:00 August 3 in CASE77f.

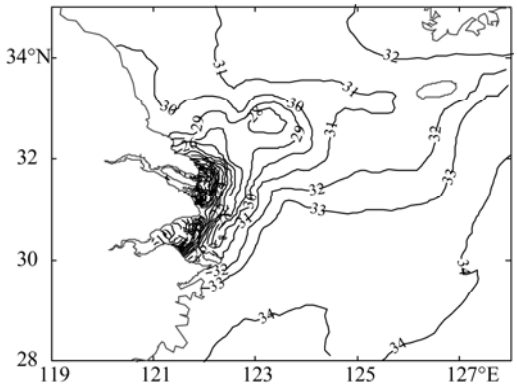

Fig. 16. Simulated surface salinity at 20:00 August 3 in CASE77g.

4.4 Effect of Taiwan Warm Current

Taiwan Warm Current (TWC), which mainly flows northeastward parallel to the 50-m isobaths from the Taiwan Strait to Tsushima-Korea Strait, is stronger in summer than in winter. In summer, it can arrive at the expansion area of CDW (Pu, 2002). Two numerical tests, namely CASE77h and CASE77i were made to analyze the effect of TWC on the LSWL.

CASE77h used the same model settings like CASE77 except that it doubled the transport of the Taiwan Strait. In CASE77h, there was an LSWL forming near the river mouth and moved to the northeast outside the CE from 11:00 July 26 to 6:00 August 11, which was similar to the LSWL in CASE77. Fig. 17 presents the characteristics of the LSWL at 20:00 August 3. Moreover, two LSWLes appeared in the northeast outside the CE later, one was from 18:00 August 13 to 1:00 August 17, and the other was from 2:00 August 22 to 14:00 August 24.

CASE77i used the same model settings like CASE77 except that it cut the transport of the Taiwan Strait in half. In CASE77i, there was an LSWL forming near the river mouth and moving to the northeast outside the CE from 13:00 July 26 to 14:00 August 11, which was similar to the LSWL in CASE77. Fig. 18 provides the characteristics of the LSWL at 20:00 August 3. Moreover, another LSWL appeared in the northeast outside the CE from 14:00 August 15 to 11:00 August 17.

The main characteristics of the LSWL can be simulated in both CASE77h and CASE77i, so TWC was not the main dynamic mechanism of the LSWL detachment, and it only slightly affected the central salinity value and the detachment time of the LSWL. CASE77h and CASE77i also confirm that TWC does not make a significant impact on the CDW because its main part is far away from the CE according to some previous studies (Zhu and Shen, 1997; Yuan *et al*., 1982).

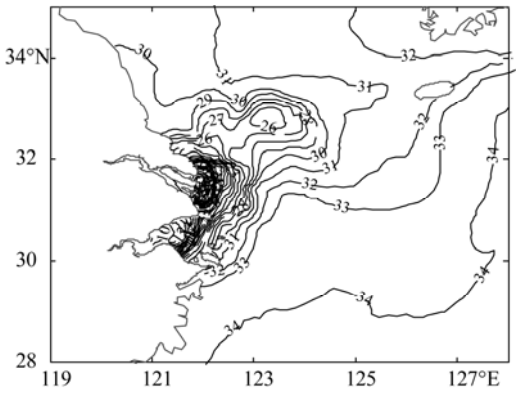

Fig. 17. Simulated surface salinity at 20:00 August 3 in CASE77h.

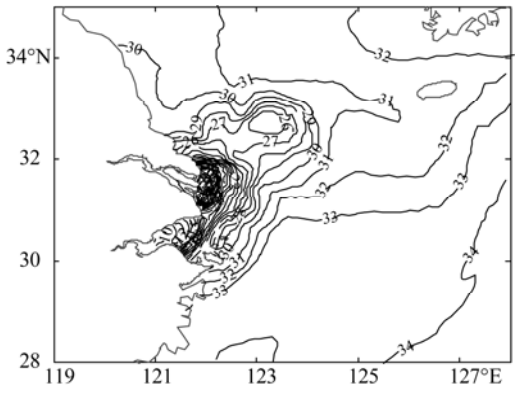

Fig. 18. Simulated surface salinity at 20:00 August 3 in CASE77i.

5. Conclusions

In this paper, POM-σ-z model is used to simulate the LSWL in summer 1977, and the simulated results indicate that LSWL was detached near the Changjiang Estuary, and then moved towards the northeast outside the CE. It remained from July 26 to August 11, its surface size was 30−130 km, and the surface salinity of its center varied from 13 to 27. The characteristics of the LSWL are similar to the observation despite some differences introduced in the third part. The sea temperature in the simulation did not change with time, which may bring errors to the simulation of the LSWL. On the other hand, there may be some errors of the LSWL described by the observation because the observed data are so limited, especially the evolution of the LSWL is not clear because continuous cruise observation is lacking. So the numerical simulation is a good way to analyze the characteristics of the LSWL, especially to analyze its evolution.

According to the analysis of the effects of wind, tide, river runoff and TWC, the wind and the tide played key roles in the formation and evolution of the LSWL in summer 1977. The main dynamic process of the LSWL is as follows: from July 22 to 26, the CDW expanded from south to north on the impact of the strong southeasterly wind with a mean speed of 6−6.5 m/s. And the vertical tidal mixing in the shallow water strengthened faster than that in the deep water from neap tide to middle tide. Thus the detachment of the LSWL occurred near the river mouth on July 26. From July 27 to 31, the continuous southeasterly wind with mean speed of 6−6.5 m/s remained, which supported the low-salinity water towards north and northeast to push LSWL northeast. Moreover, the nonuniform LRC mainly induced by wind, river runoff and density current was helpful to cut off the CDW, which was beneficial to the development of the LSWL. And at this moment, it was still in the transition from neap tide to spring tide, and thus the nonuniform vertical tidal mixing was also helpful for the development of LSWL. From August 1 to 10, the wind decreased with a mean speed smaller than 3 m/s. It has no significant effect on the enhancement or damage of the LWSL, while the horizontal tidal mixing caused the decay of the LSWL. Thus the LSWL disappeared on August 11. The hydrodynamics near

and outside the CE are very complex, and it is necessary to make further discussion on the dynamic mechanism of LSWLes in other years.

References

Blumberg, A. F. and Mellor, G. L., 1987. A description of a three dimensional coastal ocean circulation model, in: Heaps N. (Ed.), *Three-dimensional Coastal Ocean Models*, *Coastal and Estuarine Sciences*, Washington: American Geophysical Union, **4**, 1−16.

Chen, C. S., Xue, P. F., Ding, P. X., Beardsley, R. C., Xu, Q. C., Mao, X. M., Gao, G. P., Qi, J. H., Li, C. Y., Lin, H. C., Cowles, G. and Shi, M. C., 2008. Physical mechanisms for offshore detachment of the Changjiang Diluted Water in the East China Sea, *J. Geophys. Res.*, **113**, C02002, doi: 10.1029/2006JC003994.

Huang, D. J., Su, J. L. and Chen, Z. Y., 1996. Application of three-dimensional shelf sea model in Bohai. −Ⅱ The seasonal variation of temperature, *Acta Oceanologica Sinica*, **4**(1): 1−11. (in Chinese)

Liao, Q. Y., Guo, B. H. and Liu, Z. P., 2001. Analysis of direction change mechanism of the Changjiang River Diluted Water in summer, *Journal of Oceanography of Huanghai & Bohai Seas*, **19**(3): 19−25. (in Chinese)

Lie, H. J., Cho, C. H., Lee, J. H. and Lee, S., 2003. Structure and eastward extension of the Changjiang River plume in the East China Sea, *Journal of Geophysical Research*, **108**(C3): 3077, doi: 10.1029/ 2001JC001194.

Lv, X., Qiao, F., Xia, C. and Yuan, Y., 2007. Tidally induced upwelling off Yangtze River estuary and in Zhejiang coastal waters in summer, *Science in China* (*Series D*): *Earth Science*, **37**(1): 133−144.

Moon, J. H., Hirose, N., Yoon, J. H. and Pang, I. C., 2010. Offshore detachment process of the low-salinity water around Changjiang Bank in the East China Sea, *Journal of Physical Oceanography*, **40**, 1036−1053.

Pu, Y. X., 2002. The summer salinity distribution types of the 30° N profile in the East China Sea, *Donghai Marine Science*, **20**(1): 1−13. (in Chinese)

Shen, H. T., 2001. *Material Flux of the Changjiang Estuary*, Beijing, China Ocean Press, 1−7. (in Chinese)

Simpson, J. H. and Hunter, J. R., 1974. Fronts in the Irish Sea, *Nature*, **250**, 404−406.

Yuan, Y. C., Su, J. L. and Zhao, J. S., 1982. A single layer model of the continental shelf circulation in the East China Sea, *La mer*, **20**, 131−135.

Zhang,W. J., Zhu, S. X., Dong, L. X., Zhang, C. K., 2011. A new hybrid vertical coordinate ocean model and its application in the simulation of the Changjiang diluted water, *China Ocean Eng.*, **25**(2): 327−338.

Zhu, J. R. and Shen, H. T., 1997. *Expansion Mechanisms of the Changjiang Diluted Water*, Shanghai, East China Normal University Press. (in Chinese)